Neutron diffraction study of long-range atomic order in Cu-Zn-Al shape memory alloys

Neutron diffraction study of long-range atomic order in Cu–Zn–Al shape memory alloys

A Planes†, Ll Mañosa†, E Vives†, J Rodríguez-Carvajal‡, M Morin§, G Guénin§ and J L Macqueron§

† Departament d'Estructura i Constituents de la Matèria, Facultat de Física, Universitat de Barcelona, Diagonal 645, 08028 Barcelona, Catalonia, Spain
‡ Institut Laue–Langevin, BP 156 X, F-38042 Grenoble, France
§ Groupe d'Etudes de Métallurgie Physique et Physique des Materiaux and Laboratoire de Traitement du Signal et Ultrasons, Institut National des Sciences Appliquées, INSA, 20 Avenue Albert Einstein, 69621 Villeurbanne, France

Abstract. Neutron diffraction experiments have been carried out in order to investigate the ordered structures of the high temperature phase of two different Cu–Zn–Al alloys. It has been confirmed that the alloys exhibit an $L2_1$ superstructure below a critical temperature T_{c2}; a B2 superstructure between T_{c2} and T_{c1}, and a disordered BCC structure above T_{c1}.

The evolution of the degree of order has been investigated by measuring the change with temperature of the intensity of the 111 and 200 reflections. Results indicate that both transitions are second order. The critical temperatures have been determined as well as the critical exponent β. Within the experimental accuracy, it has been found that both transitions belong to the universality class of the three dimensional Ising model.

1. Introduction

A number of copper based alloys transform martensitically from BCC phases to close-packed structures [1]. The $Cu_xZn_yAl_z$ (with $0.60 < x < 0.70$) is one of such alloys and has been the subject of continued experimental and theoretical work on account of its very peculiar thermomechanical properties: shape memory effect, pseudoelasticity and high damping capacity [2], which are a direct consequence of the martensitic transition. It is well established that quantities like temperature and enthalpy change in martensitic transitions are strongly influenced by the degree of atomic order of the high temperature phase [3]. This phenomenon has been particularly studied in Cu–Zn–Al alloys because in this system the degree of atomic order is readily controllable through suitable thermal treatments [4, 5].

In spite of the extensive research carried out on Cu–Zn–Al alloys, their equilibrium ordered structure has never conclusively been established until now. Previous work showed that, at low temperature, the system exhibits a superstructure of the DO_3 or $L2_1$ type [6] (space group $Fm3m$, see figure 1). These structures can be imagined as formed by four interpenetrated FCC lattices, each one with a lattice parameter (a_F) twice the BCC lattice parameter (a_I) of the fully disordered structure (A2-type, space group $Im3m$). On increasing the temperature, the system undergoes an order–disorder transition at
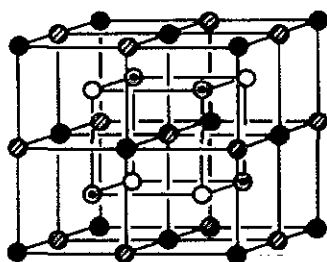
Figure 1. Unit cell of a structure of symmetry $F\bar{4}3m$, showing the definition of the four inter-penetrated FCC sublattices with Wickoff letters: (●), (4a)-1; (⊘), (4b)-2; (◉), (4c)-3; and (○), (4d)-4. In the fully ordered phase, for stoichiometries like A_3B (DO_3) or A_2BC ($L2_1$), A-atoms occupy the sublattices 3 and 4. The symmetry becomes $Fm3m$, 3 and 4 sublattices collapse in the 8c position.

T_{c2} towards a B2 superstructure (space group: $Pm3m$, lattice parameter: a_1) and further increase of temperature brings the system to an A2 structure at a transition temperature T_{c1}. The DO_3 or $L2_1$ superstructures have been detected using x-ray or electron diffraction techniques; however, alloys undergoing martensitic transitions have compositions far from the pure stoichiometric ones (A_3B for the DO_3 superstructure and A_2BC for the $L2_1$ superstructure) and therefore the aforementioned techniques are not able to provide a definitive picture of the distribution of each atomic species among the four different sublattices.

On the other hand, there have been theoretical models [7] based upon the values of ordering interaction energies determined for the different atomic pairs which suggest a most likely ground state with sublattices 3 and 4 (see figure 1) occupied by Cu atoms, one of the two remaining sublattices (1 or 2) occupied by Al and Zn and the other by Zn and Cu atoms.

The present paper is devoted to clarifying experimentally the actual situation by using neutron diffraction. This technique is specially suited for this purpose rather than x-ray or electron scattering because the scattering lengths of the three components (Cu, Zn and Al) for thermal neutrons, are different enough from each other ($b_{Cu} = 0.769\ 10^{-12}$ cm, $b_{Zn} = 0.570\ 10^{-12}$ cm and $b_{Al} = 0.345\ 10^{-12}$ cm). In addition, we have determined for the first time in these alloys the evolution of the degree of order with temperature and we have compared the measured critical temperatures with those reported in the literature for similar alloy systems obtained from electrical resistivity measurements [8]. Finally, from the evolution of the order parameter with temperature, the critical exponents for both transitions have been estimated.

The results will provide a basis for a better understanding of the peculiar thermo-mechanical behaviour intimately related to the martensitic transition in this family of shape memory alloys.

2. Experiment

Two single crystals grown by the Bridgmann method from elements of purity 99.99%, with compositions Cu–14.5 Zn–16.8 Al at.% (alloy 1) and Cu–18.9 Zn–14.5 Al at.% (alloy 2) were investigated. Cube-shaped specimens of sides about 2 mm were cut from the ingots using a low speed diamond saw. Samples were annealed for 300 s at 1070 K, slowly cooled in air and aged for several days at room temperature. After such heat treatment, the martensitic starting temperatures (M_s) were 255 K and 168 K for alloys 1 and 2 respectively.

Neutron diffraction experiments were carried out at the Institut Laue–Langevin on the four circle diffractometer (D9). The instrument has a multi-detector of 32 × 32 pixels

(each pixel covering a surface of 2 mm × 2 mm) and is equipped with a vacuum furnace. The sample–detector distance (488 mm), wavelength (0.834 Å) of the neutron beam and zero-point shifts of motors were determined by measuring a standard single crystal of Ge. Details of the detector design and performance can be found in reference [9]. The analysis of the raw data, in order to correct the integrated intensities for the Lorentz factor, was carried out by using the program described in reference [10]. A local version of the program SHELX-76 [11] was used for merging the reflections and least-squares refinements.

A set of 137 reflections up to $\sin \theta/\lambda = 1.05$ was collected at room temperature (290 K) for alloy 1. Of these reflections 76 were independent, the internal consistency index [11] was $R_{int} = 1.05\%$. For alloy 2 we measured only 76 independent reflections after verifying that the consistency was good between several equivalent reflections. The refinement of the lattice parameter gave a similar value, within the experimental error, for the two crystals: $a_F = 5.859(5)$ Å; in good agreement with previous measurements in Cu–Zn–Al system [12].

Reflections associated with the $L2_1$ (111) and B2 (200) types of ordering were measured as a function of temperature up to 950 K.

3. Results and discussion

3.1. Structure factor and room temperature ordering

The structure factor of the unit cell depicted in figure 1 can be written as a function of the effective scattering factor for each sublattice f_i $(i = 1, \ldots, 4)$. The following set of equations holds

$$f_i = \sum_\alpha x_\alpha^{(i)} b_\alpha \qquad \sum_\alpha x_\alpha^{(i)} = 1 \tag{1}$$

$$\sum_i m_i x_\alpha^{(i)} = N_c c_\alpha \qquad \sum_\alpha c_\alpha = 1 \tag{2}$$

where $x_\alpha^{(i)}$ is the fraction of the chemical species α ($\alpha =$ Cu, Zn, Al) in the sublattice i, and b_α is the Fermi length of α. N_c $(= \sum_i m_i = 16)$ is the total number of positions available in the unit cell, m_i is the multiplicity of sublattice i and c_α is the concentration of α. Concerning the values of the unit cell structure factor corresponding to the different types of ordering, three classes of reflections can be considered.

(i) h, k, l are all odd. Superstructure reflections characteristic of the DO_3 or $L2_1$ order (111, 311, 331, etc. . .):

$$F_{hkl} = 4[(f_1 - f_2) \pm i(f_3 - f_4)]. \tag{3}$$

(ii) h, k, l are all even and $(h + k + l)/2 = 4n + 2$ (n integer). Superstructure reflections characteristic of the B2 order (200, 222, 420, etc. . .):

$$F_{hkl} = 4[(f_1 + f_2) - (f_3 + f_4)]. \tag{4}$$

(iii) h, k, l are all even and $(h + k + l) = 4n$ (n integer). Fundamental reflections associated with the BCC lattice A2 order (220, 400, 440, etc. . .):

$$F_{hkl} = 4(f_1 + f_2 + f_3 + f_4). \tag{5}$$

For simplicity, in the above expressions, the Debye–Waller factors (thermal parameters) of each site are not written. From the compositions of the alloys 1 and 2

Table 1. Refinement of the crystal structure, space group $Fm3m$, of alloys 1 and 2 at room temperature. We have fixed the occupation factor of the 8c site to 0.5 (only Cu atoms). Al atoms occupy only the 4a sites. The global composition is not constrained to the nominal one. An empirical extinction parameter, E, has been refined according to the correction for the structure factor: $F_{corr} = F(1 - 0.0001EF^2/\sin\theta)$. For alloy 1, $R = 1.6\%$, extinction parameter $= 0.00017(1)$. For alloy 2 $R = 1.69\%$, extinction parameter $= 0.00032(1)$.

		$(x\,y\,z)$	Occupation numbers	$B(\text{Å}^2) = 8\pi^2 U$
Alloy 1	(4a) Al	(0 0 0)	0.181(3)	0.79(2)
	Zn		0.069(3)	
	(4b) Zn	(1/2 1/2 1/2)	0.080(4)	0.88(2)
	Cu		0.170(3)	
	(8c) Cu	(1/4 1/4 1/4)	0.5	0.95(1)
Alloy 2	(4a) Al	(0 0 0)	0.157(4)	0.92(2)
	Zn		0.093(4)	
	(4b) Zn	(1/2 1/2 1/2)	0.112(4)	0.99(2)
	Cu		0.138(4)	
	(8c) Cu	(1/4 1/4 1/4)	0.5	1.07(1)

($c_{Cu} > 0.5$) it is reasonable to assume that the ground state of long range order must have only Cu atoms in two of the four sublattices shown in figure 1. Except for degeneracies due to the choice of origin, this is equivalent to considering that sublattices 3 and 4 are occupied only by Cu atoms at 0 K. Then $f_3 = f_4 = b_{Cu}$ and F_{hkl} in (3) is real, $F_{hkl} = 4(f_1 - f_2)$, corresponding to the space group $Fm3m$. This is the main assumption we made in what follows. The approximation we have made is that the room temperature state is not very different from the ground state.

The refinement strategy we followed was based on using the same scattering factor (b_{Cu}) for the three sites: 1(4a), 2(4b) and 3(8c), allowing the refinement of the relative occupation numbers, n_1 and n_2, of sites 1 and 2, to be normalized so that n_3 was fixed at 0.5. Standard weighted least squares refinements, based on structure factors, were carried out for each crystal on 76 independent reflections. The free parameters were the two occupation numbers, three isotropic thermal parameters, the scale factor and an empirical isotropic extinction parameter [11]. The relation between n_i and f_i of equation (1) is given by $f_i = 4n_ib_{Cu}$ ($i = 1, 2$). The refined values of n_1 and n_2 are respectively 0.1323(9), 0.2292(9) for alloy 1, and 0.1394(11), 0.2210(11) for alloy 2. The parameters to be determined in our case are the four values $x_\alpha^{(i)}$ ($i = 1, 2; \alpha = $ Al, Zn) for which we have three equations (if we constrain the chemical composition to the nominal one), thus, in general, the problem is indeterminate. However, in our particular case, it is easy to verify that the refined values of n_i ($i = 1, 2$) with the conditions $x_\alpha^{(i)} \geq 0$ are only compatible with $x_{Cu}^{(1)} = 0$ and $x_{Al}^{(2)} = 0$. Putting the scattering lengths of the different species at each site and refining the occupation numbers constrained as $n_1(\text{Al}) + n_1(\text{Zn}) = n_2(\text{Cu}) + n_2(\text{Zn}) = 0.25$, we obtain the values given in table 1. It is worth mentioning that this procedure is equivalent to fitting the actual composition of the crystals. If we constrain the n_i to the nominal composition, the distribution Al + Zn in (4a), Zn + Cu in (4b) and Cu in (8c), and refine only the remaining parameters, the R-factor increases to $R = 1.8\%$ and $R = 2.24\%$ for alloys 1 and 2 respectively. The refined compositions are in good agreement with the nominal ones.
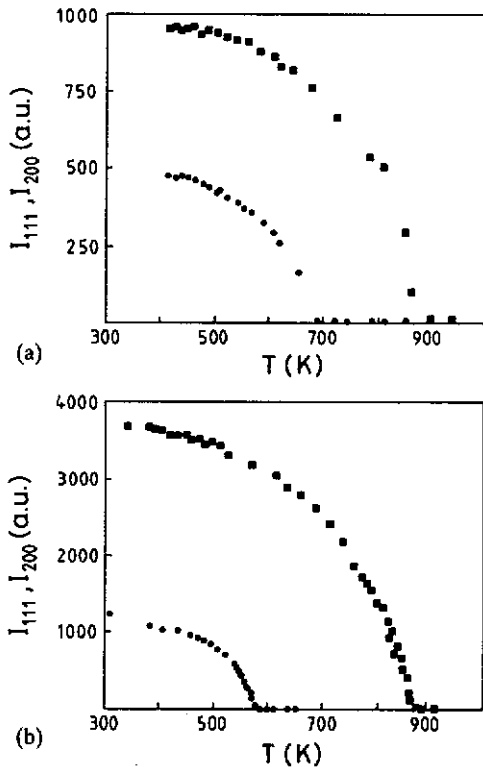
Figure 2. Temperature dependence of the (111) (●) and (200) (■) superlattice peak intensities for (a) Cu–18.9 Zn–14.4 Al at.% and (b) Cu–14.5 Zn–16.8 Al at.% alloys.
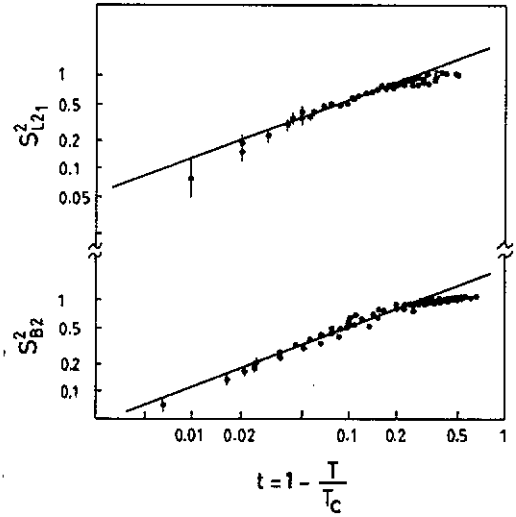
Figure 3. Log–log plot of the (111) and (200) superlattice peak intensities as a function of the reduced temperature in a Cu–14.5 Zn–16.8 Al at.% alloy.

It must be emphasized that this type of ordering corresponds exactly with the one (L2$_1$) predicted theoretically from the interaction energy between different atomic pairs [7].

3.2. Temperature dependence of the atomic order

In order to investigate the order parameter behaviour as a function of temperature, we measured the intensity of reflections (111) and (200) up to 930 K. The order parameters associated with L2$_1$ and B2 orderings verify: $S_{L2_1} \approx (f_1 - f_2) \approx (I_{111})^{1/2}$ and $S_{B2} \approx (f_1 + f_2) - (f_3 + f_4) \approx (I_{200})^{1/2}$, where I_{hkl} is the integrated intensity corrected for the Lorentz factor and the Debye–Waller factor. The number of reflections which can be collected during a heating/cooling run is limited by the heating/cooling rate. For heating/cooling rates below around 1 K min^{-1}, precipitation of equilibrium phases occurred at temperatures above about 600 K; after heating above 900 K the BCC phase was fully recovered. This precipitation of equilibrium phases compelled us to use faster heating/cooling rates which resulted in a limited number of reflections collected in a complete run.

Figure 2 shows the evolution with temperature of the intensity of 111 and 200 peaks for the two alloys investigated. Measurements were carried out while the temperature

of the sample was continuously changing but collection of some reflections at constant temperature—far from the precipitation range—ensured that data were not affected by the heating/cooling rate.

Since the sample had to be cooled/heated fast enough to avoid precipitation of equilibrium phases, collection of several independent reflections at different temperatures was not feasible. For this reason the evolution of the Debye–Waller factor with temperature was estimated from the evolution of the intensity of the fundamental 220 peak, collected at some different temperatures within the working range. Also, the intensity of 220 peaks was used to verify that no precipitation occurred during heating/cooling runs.

From figure 2 we have estimated the critical temperatures $T_{c1} = 860 \pm 10$ K and $T_{c2} = 660 \pm 10$ K for the alloy 1 and $T_{c1} = 880 \pm 5$ K and $T_{c2} = 585 \pm 5$ K for alloy 2. Rapacioli and Ahlers [8] used electrical resistivity measurements to obtain the critical temperatures for a wide range of compositions in Cu–Zn–Al alloys. Present results fit well on their curves for T_{c2}; but the neutron scattering experiments give slightly higher values for T_{c1}.

It is worth pointing out that T_{c2} is much more sensitive to the composition than T_{c1}, also, the difference in T_{c2} (75 K) is similar to the difference in M_s (83 K) for both samples. Indeed, a good correlation between martensitic transformation temperatures and $L2_1$ ordering temperatures has been already reported by Murakami [13] for the Au–Zn–Cu alloy.

From figure 2 it seems apparent that both order–disorder transitions are of second order. For alloy 2 we performed several heating/cooling runs so that a large number of 111 and 200 reflections were collected close to the transition points. As indicated previously, after the pertinent corrections, the integrated intensity behaves as the square of the order parameter (S) which, near T_c, must obey the power law:

$$S = At^\beta \tag{6}$$

where t is the reduced temperature $1 - T/T_c$. We have estimated the critical exponent β by performing a log–log fit of the intensity versus the reduced temperature. This plot is shown in figure 3. Data correspond to different heating and cooling runs for two different samples of the same alloy. A least-square fitting procedure has been used, weighted by the inverse of the square of the relative error associated with each data point; the best fit is also plotted in figure 3. For the B2 to $L2_1$ transition we have obtained $\beta = 0.315(15)$ and $A = 1.51(6)$ and for the B2 to A2 transition, $\beta = 0.320(20)$ and $A = 1.48(8)$. These values are consistent with the theoretical estimate $\beta = 0.312$ and $A = 1.506$ [14] for a three-dimensional Ising model.

Our present results are consistent with previous measurements of the β exponent for the B2 to A2 transition in Cu–Zn alloy [15] and for the DO_3 to $L2_0$ transition in Fe_3Al [16] alloys. It must be stressed that our investigations have been carried out in ternary alloys exhibiting two successive order–disorder transitions.

4. Conclusions

Below T_{c2}, Cu–Zn–Al exhibits an $L2_1$ order with the following distribution of atoms into sublattices (see figure 1): sublattice 1 occupied by atoms of Al and Zn, sublattice 2 occupied by atoms of Cu and Zn; sublattices 3 and 4 fully occupied by atoms of Cu.

The degree of atomic order at each temperature has been determined for the first time in Cu–Zn–Al alloys. Both A2 to B2 and B2 to L2$_1$ transitions are continuous and are members of the three-dimensional Ising model universality class.

Acknowledgments

References

[1] Warlimont H and Delaey L 1974 *Prog. Mater. Sci.* **18** 1
[2] Delaey L, Krishnan R V, Tas H and Warlimont H 1974 *J. Mater. Sci.* **9** 1536
[3] Planes A, Viñals J and Torra V 1983 *Phil. Mag.* A **48** 501
[4] Rapacioli R and Ahlers M 1979 *Acta Metall.* **27** 777
[5] Planes A, Romero R and Ahlers M 1990 *Acta Metall.* **38** 757
[6] Chakravorty S and Wayman C M 1977 *Acta Metall.* **25** 989
[7] Ahlers M 1986 *Prog. Mater. Sci.* **30** 135
[8] Rapacioli R and Ahlers M 1978 *Scr. Metall.* **11** 1147
[9] Lehmann M S, Kuhs W E, McIntyre G J, Wilkinson C and Allibon J R 1989 *J. Appl. Cryst.* **22** 562
[10] Wilkinson C, Khamis H W, Stanfield R F D and McIntyre G J 1988 *J. Appl. Cryst.* **21** 471
[11] Sheldrick G M 1976 *SHELX-76: program for crystal structure determination* University of Cambridge
[12] Guénin G, Pynn R, Rios–Jara D, Delaey L and Gobin F P 1980 *Phys. Status Solidi* a **59** 553
[13] Murakami Y 1972 *J. Phys. Soc. Japan* **33** 1350
[14] Essam J W and Fisher M E 1967 *J. Chem. Phys.* **38** 802
[15] Norvell J C and Als–Nielsen J 1970 *Phys. Rev.* B **2** 277
[16] Guttmann L, Schnyders H C and Arai G J 1969 *Phys. Rev. Lett.* **22** 517